Industrial Engineering Journal
ISSN: 0970-2555
Volume : 52, No. 2, JULY - DECEMBER 2023

A Deign of Nonparametric Spectral Analysis for Movement Identification in Encephalography Signals

T.Bhavani[1], S.Naresh[2], K.Srikanth[3], M.Ganesh[4]T.Divya[5],M.Srilatha [6]

[1,2,3,4,5,6] Assistant Professor, Department of ECE, Sri Indu Institute of Engineering & Technology, Hyderabad

Abstract: ***The purpose of the following study is to determine patterns generated by 6 movements: Opening / Closing - Eye, Opening / Closing-Mouth, Concentration, Meditation, Eye Movement Up / Down, and Left / Right Eye Movement recorded in the prefrontal area in the pointN_z, applying nonparametric spectral estimation techniques, using the Fast Fourier Transform (FFT), Barlett's Periodogram, and Welch's Periodogram. For this purpose, the measurements were made externally to 30 subjects in the age range of 18 to 22 years, taking as reference 200 sessions per movement applying 10 seconds of test. The sampling frequency in the recording was equal to$F_s = 512\ Hz$. The results show sampling frequencies in the range of the Delta 0.5-3.5Hz biosignal applying the FFT method and Bartlett's Periodogram, Welch's Periodogram is not recommended for use by applying a rectangular window greater than 4, generating attenuation in the harmonics.***

Keywords: EEG, Nonparametrics methods, Delta Biosignal, Prefrontal surface

1. Introduction

Studies estimate patterns generated by brain activity leading to tests called Electroencephalogram (EEG) using surface or basal electrodes, Electrocorticogram (ECoG) implementing surgical electrodes on the surface of the cerebral cortex, and Stereo Electroencephalogram (E-EEG) using surgical electrodes of deep application. Surgical tests such as ECoG and E-EEG [1], [2] have presented a better visualization in the collection of samples in the brain bioelectric activity, however, the surgical application of the electrodes entails a high-risk, high-cost process, and difficulty in the application. The main objectives of EEG studies are focused on the biomedical area to find abnormalities such as dyslexia, epilepsy, psychological symptoms [3], [4], [5] stress tests in adults and children as mentioned [6], sleeplessness [7], concentration level [8] and a lower percentage in the study of movements, for this the main solution focuses on developing electrodes with low loss, reusable and easy to apply no matter the cost of acquisition. In the present study, a dry contact electrode made of Chloride Silver with an accuracy of 95% comparing its response with surgical electrodes will be adapted. Results applying spectral estimation techniques in encephalographic tests have shown the noise immersed in frequencies above 50 Hz [9],[10] and the frequency relationship of the bioelectric signals categorizing 7 basic signals concerning the known operating frequency: Delta (1-3 Hz), Theta (4-7Hz), Alpha (8-13 Hz), Low Beta (12-15 Hz), Mid Beta (16-20Hz), High Beta (21-30 Hz) and Gamma ($\leq$ 30 Hz) mentioned in [11], [12]. Previous investigations have been generated in the determination of the flicker considering the result of slow harmonics with narrow peaks in the range of 0.5 to 7 Hz. However, no related theory has been found in the spectral estimation executing movements of Opening/ Closing of the Mouth, Movement Upper/ Lower ocular, Left/ Right eye movement, Deep meditation and Concentration applying spectral estimation techniques such as the Fast Fourier Transform (FFT), Bartlett Periodogram and Welch Periodogram categorized as nonparametric methods of spectral estimation [13]. In the present study the results obtained will be shown when applying the 3 types of techniques in each movement visualizing the trend of the spectrum in the course of time (sessions) [9], frequencies with maximum weights per session and maximum harmonic variance, focusing the results in the determination of the most suitable nonparametric technique for each movement.

2. Material and methods

The population studied consists in thirty subjects from 18 to 22 years, not considering sex or physical characteristics. They were tested by performing 6 facial movements capturing 30 sessions per movement in a span of 10 seconds per session. The data capture is based on a dry (external) electrode where [14] mentions the potential of the device at points C3 and C4, in this study the electrode was placed at the $N_z$point in the prefrontal area using the International System (SI) 10/20 [15], [4] referenced by the left lobe [11]. Each movement involved 300 seconds of continuous tests with breaks of 36 seconds per session obtaining a total of 23 minutes per movement and 138 minutes per subject. The conditioning of the signal $x(n)$ was done applying a Butterworth Low-Pass filter of $-60\ dB$ followed by an Amplification and Conversion A / D stage [1], the sampling frequency (F_s) was equal to

Industrial Engineering Journal
ISSN: 0970-2555
Volume : 52, No. 2, JULY - DECEMBER 2023

$512\,Hz$ computing with a resolution of 16 Bit's. Based on the Discrete Fourier Transform (DFT) characterized by

$$X(\omega) = \sum_{n=-\infty}^{\infty} x(n)e^{-j\,\omega n} \quad (1)$$

Where $X(\omega)$ represents the frequency vector bounded in $(-\infty, \infty)$, $x(n)$ represents the brain signal converted in time (t) to samples (n) through a preprocessing stage. The expression $e^{-j\,\omega n}$ is represented in practical cases as

$$e^{-j\alpha} = \cos(\alpha) - jsen(\alpha) \quad (2)$$

2.1. Linear Transformation in Discrete Fourier Transform (DFT)

The model visualized in (1) is linearized the expression as

$$X(k) = \sum_{n=0}^{N-1} x(n)W_N{}^{kn}, k = 0,1\ldots, N-1 \quad (3)$$

$$W_N = e^{\frac{-j\,2\pi}{N}} \quad (4)$$

In the previous equation N is the length of the sample vector (n), $\boldsymbol{W}_N$ is the complex matrix of dimension NxN represented as

$$W_N = \begin{bmatrix} 1 & 1 & 1 & \ldots & 1 \\ 1 & W_N & W_N{}^2 & \ldots & W_N{}^{N-1} \\ 1 & W_N{}^2 & W_N{}^4 & \ldots & W_N{}^{2(N-1)} \\ \vdots & \vdots & \vdots & \ldots & \vdots \\ 1 & W_N{}^{N-1} & W_N{}^{2(N-1)} & \ldots & W_N{}^{(N-1)(N-1)} \end{bmatrix} \quad (5)$$

The expression (3), (4) and (5) is simplified making a series obtaining the generalized terms in the analysis carried out, as shown below

$$X(0) = x(0)e^{\frac{-j\,2\pi(0)(0)}{N}} + x(1)e^{\frac{-j\,2\pi(1)(0)}{N}} + \cdots + x(N-1)e^{\frac{-j\,2\pi(N-1)(0)}{N}}$$

$$X(1) = x(0)e^{\frac{-j\,2\pi(0)(1)}{N}} + x(1)e^{\frac{-j\,2\pi(1)(1)}{N}} + \cdots + x(N-1)e^{\frac{-j\,2\pi(N-1)(1)}{N}} \quad (6)$$

$$X(2) = x(0)e^{\frac{-j\,2\pi(0)(2)}{N}} + x(1)e^{\frac{-j\,2\pi(1)(2)}{N}} + \cdots + x(N-1)e^{\frac{-j\,2\pi(N-1)(2)}{N}}$$

$$\vdots$$

$$X(N-1) = x(0)e^{\frac{-j\,2\pi(0)(N-1)}{N}} + x(1)e^{\frac{-j\,2\pi(1)(N-1)}{N}} + \cdots + x(N-1)e^{\frac{-j\,2\pi(N-1)(N-1)}{N}}$$

To compute the expression (6) it is used the trigonometric expressions changing $e^{\frac{-j\,2\pi nk}{N}} = \cos(\frac{-2\pi nk}{N}) + jsen(\frac{-2\pi nk}{N})$ obtaining the graph of magnitude $|X(k)|$ and phase of the spectrum $\angle X(k)$.

2.2. Fast Fourier Transform (FFT)

The application of the FFT has been the most common method in spectral analysis, as mentioned in [16], [11], [15]. In this section, the application was based on the base 2 algorithm in the vector $x\,(n)$ with N equal to 5120 samples adding zeros in relation to the nearest base 2 of the vector 8192 samples. The results were computed through expressions

$$X(k) = \sum_{n=0}^{N-1} x(n)W_N^{kn}, k = 0,1,\ldots, N-1 \quad (7)$$

$$X(k) = \sum_{n\,par} x(n)\,W^{kn} + \sum x(n)\,W_N^{kn} \quad (8)$$

$$\sum_{m=0}^{(\frac{N}{2})-1} x(2m+1)W_N^{k(2m+1)} \quad (9)$$

Expression (8) shows the division of the DFT into two subsets with $N/2$, where $n\,par$ specifies the set of even samples and $n\,odd$ the odd samples, generating two $F_1(k)$and $F_2(k)$when performing the technique of processing. The symmetry properties allow the conversion$W_N^2 = W_{N/2}$, proposing the expression (9) as

$$X(k) = \sum_{m=0}^{(\frac{N}{2})-1} f_1(m)W_{\frac{N}{2}}^{km} + \cdots$$

$$W_N^k \sum_{m=0}^{(\frac{N}{2})-1} f_2(m)W_{\frac{N}{2}}^{km} \quad (10)$$

$$F_1(k) + W_N^k F_2(k), \quad k = 0,1,\ldots, N-1 \quad (11)$$

The data length is transformed by two data vectors $f_1(m)$and $f_2(m)$obtaining two DFT with a shorter processing time, reducing $0 \le m \le N/2$. The previous relationship contemplates the following process

$$X(k) = F_1(k) + W_N^k F_2(k), \ldots \quad k = 0,1,\ldots, \frac{N}{2} - 1 \quad (12)$$

$$X(k + \frac{N}{2}) = F_1(k) - W_N^k F_2(k), \ldots \quad k = 0,1,\ldots, \frac{N}{2} - 1 \quad (13)$$

2.3. Power Spectral Density

The Power Spectral Density (PSD) expressed as E represents the area under the curve of a signal in time (t) by raising its absolute value squared in all $t \in (-\infty, \infty)$ when finite energy $< \infty$, the expression is given as

$$E = \int_{-\infty}^{\infty} |X_a(t)|^2 dt < \infty \quad (14)$$

The result of finite energy in a sampled vector contemplates the existence of its DFT, as specified below

$$X_a(F) = \int_{-\infty}^{\infty} x_a(t)e^{-j2\pi Ft}\,dt \quad (15)$$

applying Parseval's Theorem in (15) it is corroborated that the power of the signals is equivalent to the sum of the power in their spectral components, agreed with [18].

$$E = \int_{-\infty}^{\infty} |x_a(t)|^2 dt = \int_{-\infty}^{\infty} |X_a(F)|^2 dF \quad (16)$$

$$S_{xx}(F) = |X_a(F)|^2 \quad (17)$$

Where $S_{xx}\,(F)$ represents the sum of the harmonics expressed in spectral power and$|X_a\,(F)|^2$is the squared modulus of the Fourier transform of the vector$x_a\,(t)$. Another path defined in the obtaining of the PSD is based on the Autocorrelation function$R_{xx}\,(r)$, being the result of the multiplication of two functions where $x_a(t + r$represents the displacement in τ of the sampled vector, the expression (18) details at [18]. It is finalized by obtaining the DFT of the Autocorrelation function [11] evaluating it

Industrial Engineering Journal
ISSN: 0970-2555
Volume : 52, No. 2, JULY - DECEMBER 2023

N $n\ impar$ N in the interval $(-\infty, \infty)$ by means of the definite integral.Equation (19) specifies the spectral power obtained by each movement by applying the DFT.

$$X(k) = \sum_{m=0} x(2m)W_N^{2mk} + \cdots$$

Industrial Engineering Journal
ISSN: 0970-2555
Volume : 52, No. 2, JULY - DECEMBER 2023

$$R_{xx}(r) = \int^{\infty} x^*(t)x\ (t+r)dt \quad (18)$$

$$S_{xx}(F) = |X_a(F)|^2 = \int_{-\infty}^{a}{}^{a}_{\infty} R_{xx}(r)e^{-j2\pi Fr}\,dr \quad (19)$$

2.4. Barlett´s Periodogram

The reduction of the variance is based on subdividing the data sequences $x(n)$ into several non-overlapping windows M by superimposing the windows when applying the DFT. The data vector $x_i(n)$relates a segment of the vector $x(n)$within a range $0 \le n \le M-1$. A defined periodic signal would express a defined weighted average, the weak encephalographic signals show non-permanent cycles with varying frequency weights determined as noise [10] decreasing the harmonics eliminated by means of the averaged

$$P^{(i)}{}_{xx}(f) = \frac{1}{M}\left|\sum_{n=0}^{M-1} x_i(n)e^{-j2\pi fn}\right|^2, \ldots$$
$$i = 0,1,\ldots,K-1 \quad (20)$$

$$P^{B}_{xx}(f) = \frac{1}{K}\sum_{i=0}^{K-1} P^{(i)}_{xx}(f) \quad (21)$$

The expression (20) shows the calculation of the periodogram by segments, where $P^{(i)}{}_{xx}(f)$represents the PSD in each segment of length M, denotes the application of the DFT in the expression $x_i(n)e^{-j2\pi fn}$. The Bartlett periodogram is expressed in equation (21) where $P^{B}{}_{xx}(f)$represents the average PSD of each segment i from $0 \le i \le K-1$for all windows with data length M.

$$E[P^{B}{}_{xx}(f)] = \frac{1}{K}\sum_{i=0}^{K-1} E[P^{(i)}{}_{xx}(f)] = E[P^{(i)}{}_{xx}(f)] \quad (22)$$

2.5. Periodograma de Welch

The result presented in the previous section shows the application of Barlett's Periodogram (Without overlapping). The estimation of the Welch method represents an overlap and a windowing to obtain the average of the Power Spectrum [18] represented as follows:

$$P^{(i)}{}_{xx}(f) = \frac{1}{MU}\left|\sum_{n=0}^{M-1} x_i(n)w(n)e^{-j2\pi fn}\right|^2, \ldots$$
$$i = 0,1,\ldots,L-1 \quad (23)$$

The expression $P^{(i)}{}_{xx}(f)$ represents the Modified Welch Periodogram, M the length of the segment window, U the normalization factor for the power of the window function ending with $w(n)$ representing the window. Obtaining the constant U is obtained by calculating the average of the values of the window squared between the data number M expressed as:

$$U = \frac{1}{M}\sum_{n=0}^{M-1} w^2(n) \quad (24)$$

The set of segments is averaged overlapping Bartlett's Periodogram products with the window, obtaining the PSD.

$$P^{W}_{xx}(f) = \frac{1}{L}\sum^{L-1} \tilde{P}^{(i)}_{xx}(f) \quad (25)$$

more dissipated spectrum eliminating the low amplitude harmonics.

$$E[P^{W}{}_{xx}(f)] = \frac{1}{L}\sum_{i=0}^{L-1} E[\tilde{P}^{(i)}{}_{xx}(f)] \quad (26)$$

$$E[P^{W}{}_{xx}(f)] = E[\tilde{P}^{(i)}{}_{xx}(f)] \quad (27)$$

The distributions of the Energy in the harmonics are considered as the average of the modified Periodogram named as $E[P^{W}{}_{xx}(f)]$ in the expression (26). The expanded equation of the Periodogram is specified in (27).

$$E[\tilde{P}^{(i)}{}_{xx}(f)] = \frac{1}{MU}\sum_{n=0}^{M-1}\sum_{m=0}^{M-1} w(n)w(m)E[x_i(n)x^*_i(m)]e^{-2j\pi f\ (n-m)} \quad (28)$$

3. Results and Discussion

3.1. Raw Signal and FFT processing

Figure 1 shows the biosignals in magnitude $(\mu V)$and Time (s) when performing the 6 movements known as a RAW signal, no previous preprocessing stage was performed in the development of the analysis, and the concentration and meditation tests do not visualize patterns direct [1].The tests carried out do not show upper and lower amplitudes in the range of 600 μV to $-600\ \mu V$, the synchronization of the equipment delays the recorded signal 1.2 Seg, proposing to visualize 8 complete Segs. Figure 1(a) contains Delta, Theta and Alpha components, each flashing is specified as a high-weighting cycle (V_{max}) and low (V_{min}), the concentration of the subject is measured between the span of each opening obtaining variations within the 100 to -100µV range. Figure 1(b) presents variations within two overshoots, the first overshoot specifies the movement when making the lock in the mouth causing variations by the pressure of the muscles zygomatic major, zygomatic minor, risorio, platysma and depressors, the overshoot it ends when the mouth is opened, relaxing the muscles, decreasing the pressure, the described phenomenon is visualized in the seconds 0 to 4. The Figure 1(c) focuses on the variations produced by the concentrated subject where a range in amplitude is obtained within 150 to $-50\mu V$, the results do not specify dominant harmonics or spectral trends in the sessions, contributing as a primary characteristic to the constant variability of the subject without weights in the sampled signal $x(n)$.The decrease in magnitude was considered in Figures 1(c) and (d) by limiting the range to 250 to - 50 µV.The Figure 1(e) maintains a trend compared to Figure 1(a) the maximum positive impulse maintains an amplitude of 600 μV, while differing in the amplitude of the reverse peak maintaining a value close to $-200\ \mu V$, each overshoot emphasizes less narrow lobes [9] visualizing concentrations in the intervals of change in potential. Figures 1 (a), (e) and (f) present convolutions with different amplitude variations, atypical amplitudes are visualized, and the quality of the signal in the current test is linked to the test subject in most situations a signal was obtained with a noise similar to the concentration with minimal deformations representing the Left / Right eye

Industrial Engineering Journal
ISSN: 0970-2555
Volume : 52, No. 2, JULY - DECEMBER 2023

$i=0$

The term of the equation (25) $P_{xx}^{W}(f)$ is the result of the Welch periodogram in PSD estimating the harmonics
present in the spectrum, the smoothing given to the set ofaverages made and the product of the window generates a movement. The process shown in equations (1) to (19) wasconcretized in the obtaining of the spectral analysis where
$S_{xx}(F)$is specified in dB obtaining it given the relation of $10log_{10}$in the power spectral density(PSD). Figures 2 presents the best seconds per test performed on 30 subjects, applying 200 tests for each movement. Figures 2(a) shows the overlapping evolutions and harmonics to observe the effect of the average PSD in all sessions in Delta, the yellow dotted line specifies the average of each test obtaining 4 weighted frequencies found in $f_1 = 0.2Hz$, $f_2 = 0.7\,Hz$,
$f_3 = 1.2\,Hz$ and $f_4 = 1.7\,Hz$ in the frequency range of $0.5\ a\ 2\ Hz$ the tests show similarity throughout the course in frequency $X(\omega)$, in higher frequencies variations of random brain activity (concentration) are obtained.

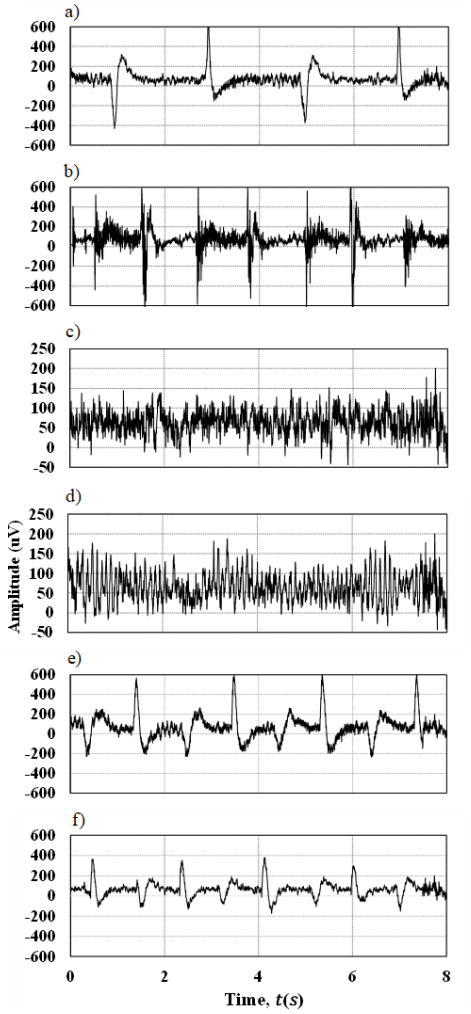

Figure 1: Real signals in the 6 movements captured in subject 1: a) Opening/Close-Eye, b) Opening/Close-Boca, c)Concentration, d) Meditation, e) Up/Down-Eye y f) Left/Right-Eye

The Figure 2(b) focuses on abrupt variations maintaining a margin in the estimation of the range in frequency and amplitude in PSD, the interacting harmonics are found in $f_1 = 0.9\ Hz$, $f_2 = 1.8\ Hz$ and $f_3 = 2.7Hz$, the assiduity specifies multiples in frequency, the components show greater biopotentials in the range of the Delta biosignals [16], and in higher frequencies the level of negative PSD decreases. Figure 2(c) shows non-point random encephalic
activity in the determination of the concentration, a quasi- null average is visualized given the variance of the samples, and the variations shown in the graphs show a range in PSD (dB) in 10 a$-10dB$, in the Theta, Alpha, Low Beta, Mid Beta, High Beta ranges maintains similar weightings, frequencies greater than 30 Hz [20], [21] in the Gamma range the signal decrement is displayed, in the points C3 and C4 weights have been found at 20 Hz [14]. Figure 2(d) locates harmonics in the Alpha range obtaining variations in frequency in the range of 9.6 to 11.6 Hz, lower frequencies do not show point harmonics to obtain a reference in the spectrum, frequencies greater than 11.6 Hz decrease in magnitude, lower at 9.6 Hz they remain constant obtaining similarity with the concentration. In the Figure 2(e) present a distinction in harmonics in relation to Figure 2(a), as it´s observed in the raw signal visualizing Figure 1(a) the samples of the data vector $x(n)$ specify a similar pattern, the main difference lies in its frequency components obtaining harmonics in $f_1 = 0.5\ Hz$, $f_2 = 1.5\,Hz$ and $f_3 = 2.5\,Hz$
shown in the averaged signal, the ponderations show an increase of 1 Hz in each interval, confirming a multiple in frequency, the PSD (dB) is within the range of 18.4 to $-10dB$, the harmonics are found in the Delta biosignal. The Figure 2(f), does not present harmonics defined in the average signal Left / Right eye movement presents a high concentration factor, in tests performed, a value greater than 95% of subjects presented a large number of unwanted variations, visualizing in Figure 1(f) the sample vector of 10 subjects considered as remaining 5% obtaining a good visualization, The Figure 2(c), (d) and (f) show harmonics with different working ranges [19], The Figure 2(f) presents amplitudes in PSD(dB) of $5 - 10\ dB$ focused in Delta biopotential, the frequency ranges were limited, frequencies greater than 3.5 Hz the magnitude decreases.The results present below show the spectral variations $X(\omega)$ over the time course (t) of the sample, taking the frequency range Delta as a reference.

Industrial Engineering Journal
ISSN: 0970-2555
Volume : 52, No. 2, JULY - DECEMBER 2023

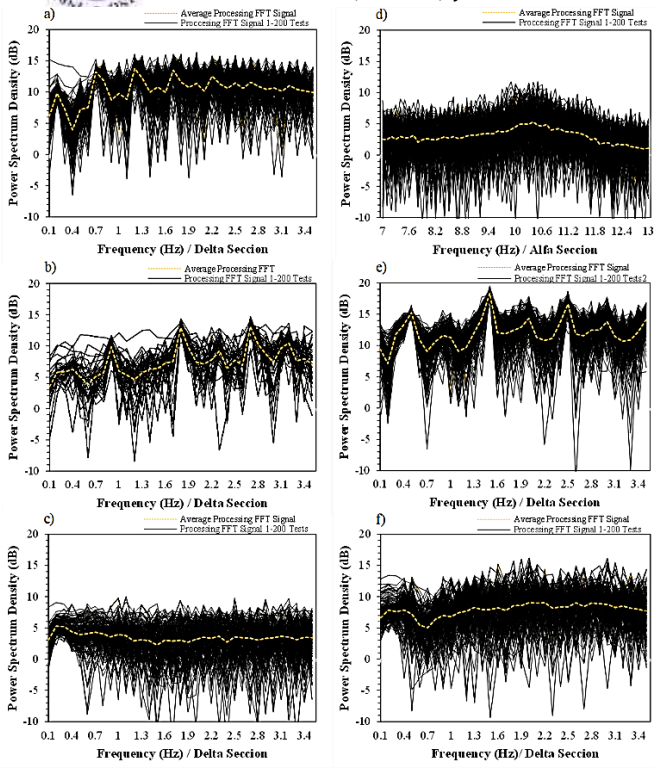

Figure 1: Processing by applying Fast Fourier Transform in6 movements in 200 tests in 10 Seg ($N = 5120, 0.5 \leq \Delta \leq 3.5\ Hz$, $7 \leq \alpha \leq 13\ Hz$-Meditation): a) Opening/Close-Eye, b) Opening/Close-Boca, c) Concentration, d) Meditation, e)Up/Down-Eye y f) Left/Right-Eye.

Figure 3(a) shows the flickering movement or Opening / Closing - Eye interacting 3 weighted frequencies obtaining the same energy in PSD (dB) of $|X_a(f)|^2$, the tests do not present deformations over time in the slow wave frequencies. Figure 3(b) represents the Opening / Closing Movement - Mouth obtaining two weights with a straight trajectory throughout the spectral harmonic, the openings and closures with the greatest magnitude are generated by Delta harmonics in the range of $0.5\ a\ 1.5Hz$.

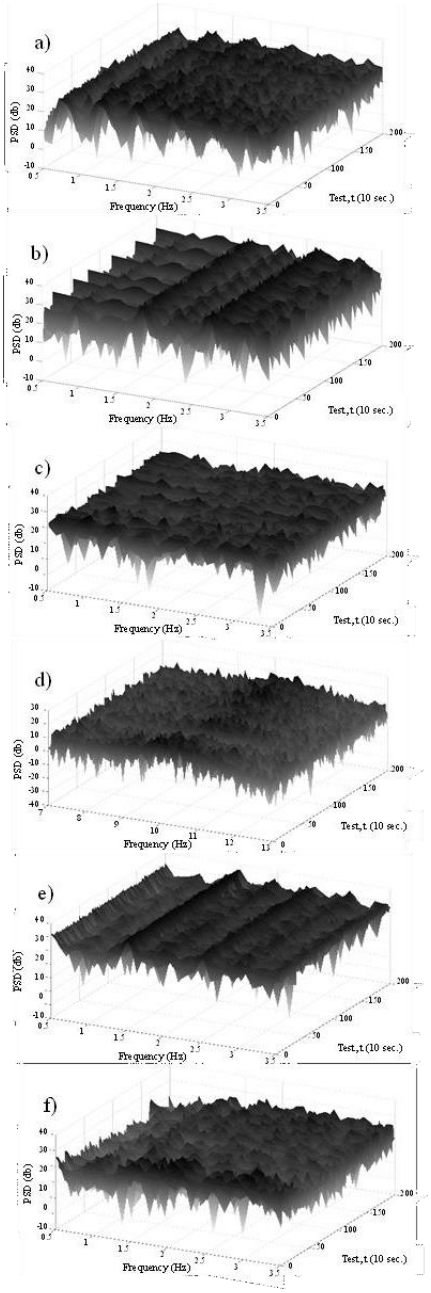

Figure 2: Pseudo-tridimensional graphic of evolution in frequency - FFT: a) Opening/Close-Eye, b) Opening/Close-Boca, c) Concentration, d) Meditation, e) Up/Down-Eye y f) Left/Right-Eye Figure 3(c) shows the concentration in the subjects visualizing a set of variant harmonics with a scaled spectral density, the results obtained by [22] show similarity in the temporal course, some sessions have higher energy PSD(dB) given the ease in subject concentration and brain activity shown by highlighting tests0 a 21, 50, 103, 165 y 199. Theobservation range was modified in Figure 3 (d) showing the harmonics in the Alpharange of the Meditation test [23], There is a set of harmonicswith high PSD (dB) magnitudes compared to the tests shown in Figure 3(a), (b) and (c), the Delta range was not considered as a consequence of flat surfaces (no variants). Figure 3(e) represents the movement of Up / Down-eyemovement achieving two obvious harmonics characterizing the upper movement of the eyepiece as the higher frequency (f_{max}) and

Industrial Engineering Journal
ISSN: 0970-2555
Volume : 52, No. 2, JULY - DECEMBER 2023

lower movement of the eyepiece (f_{min}). Figure 3(f) show the movement left/right-eye movement characterized by the mean of two frequencies with magnitudes close to concentration.The movement frequency values are subtle and do not display distinguishable patterns, confusing their harmonics in frequency with Concentration or Meditation [1].

3.2. Bartlett's periodogram processing

The modification implemented in the DFT shown in (1) - (19) implemented the modification by Barlett in segments asspecified in (20)-(22) obtaining a magnitude in
$PSD(dB)$greater in $E[P^B{}_{xx}(f)] \geq S_{xx}(f)$. Figure 4 shows the spectral analysis overlapping the samples made by the 30 subjects as was done with the FFT in two-dimensional graphics, the range of operation of the spectrum is at $40\ a - 10\ dB$ in the Eyes Open / Close tests and Eye
Movement Up / Down, the spectra did not suffer visual distortions in the average frequency, the representations of the graphs were determined by sessions of 10 seconds. A better visualization was obtained in the range of the Delta biosignal in $0.5 - 3.5\ Hz$ with the exception of Alpha within $7 - 13\ Hz$ in Meditation. Some graphs do not show significant frequency evolutions, determining the movements according to their range in amplitude. Figure 4(a) implements Barlett's Periodogram spectral techniquewith 2 segments, with a segment length equal to $M = 2560$, determining if there is variation in the final averaging in each stage, the 200 tests performed show no significant deformation in the average signal with harmonics in 0.7,1.2 y 1.7 Hz as obtained in Figure 2(a).The graph shown in Figure 4(b) does not show differences in components comparing the result with the FFT, the maximum magnitude
PSD_{max} implied by the averaged signal is 32.81 dB. Figures 4(c), (d), (e), and (f) show the same harmonics with changes in amplitude with respect to Figures 2(c), (d), (e) and (f) in the Delta frequency range, both techniques show similar behavior in the 6 movements, smoothing occurs at higher frequencies directed to harmonics in Theta to Gamma, isolating the phenomenon of Meditation decreasing its
magnitude at higher frequencies of the Theta biosignal. Figure 5(a) maintains the pattern found in Figure 2(a) with the difference in the spectral density, the harmonics evolved in time show the same linear trajectory in all the sessions, and the averaging of the 2 segments does not show an important variation in the decrease of the concentration signal compared to the FFT in the Delta section. Figure 5(b) represents the most smoothed set of frequencies with respect to Figure 2(b), the negative increments denote an attenuated PSD (dB) due to K factor.

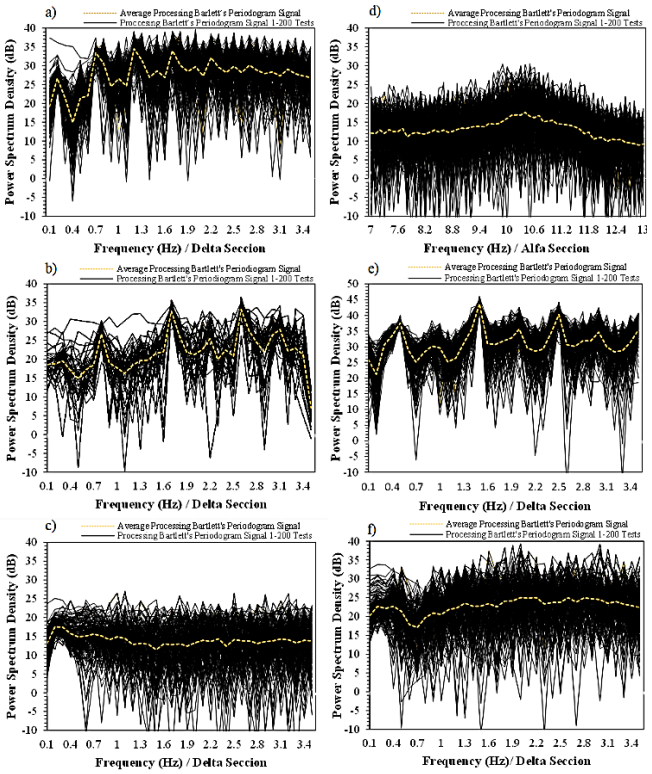

Figure 3: Processing by applying Barlett´s Periodogram in 6 movements in 200 tests in 10 Seg (N=5120,0.5≤Δ≤3.5 Hz, 7≤α≤13 Hz-Meditation): a) Opening/Close-Eye, b) Opening/Close-Boca, c) Concentration, d) Meditation, e) Up/Down-Eye y f) Left/Right-Eye.

Following the Figure 5(c) shows a similar phenomenon to the processing of the FFT with significant attenuation in the outstanding harmonics, the process does not show a set of harmonics with relevant temporal evolution, however, the result is similar to other techniques focusing on frequencies in $0.5\ to\ 3.5\ Hz$ obtaining the largest amplitude of dB as mentioned [23], no destructive attenuation is generated, as specified in [22]. The range of operation in Meditation is visualized in Figure 5(d) expresses point harmonics with semilinear time evolution, obtaining results that vary arounda range in operation frequency, as verified in Figure 4(d) variations increased in magnitude, a smaller number of tests denote smoothing in negative magnitudes. Figures 5(e) and (f) do not show significant changes in better visualization of the spectrum, they maintain proportion in amplitude in comparison with Figures 2(e) and (f) the harmonics do not show changes in frequency. The implementation of the Bartlett Periodogram with 2 segments did not obtain a better result compared to the FFT, the averaging of the alpha biosignal, Low Beta, Mid Beta, High Beta, and Gamma was not attenuated by applying two segments.

3.3. Application and selection of window in Welch Periodogram

The selection of the technique was performed by comparing the individual frequency response of test 1 for the Opening /

Industrial Engineering Journal
ISSN: 0970-2555
Volume : 52, No. 2, JULY - DECEMBER 2023

Closing movement - Eye showing the working range of the Delta biopotential, Figure 6(a) comparing each window
w (n) Rectangular with each Welch Periodogram applying different segments.The test was carried out applying Welch's Periodogram method for an even number of 2,4,8,16 and 32 in relation to Barlett's Periodogram and the FFT.

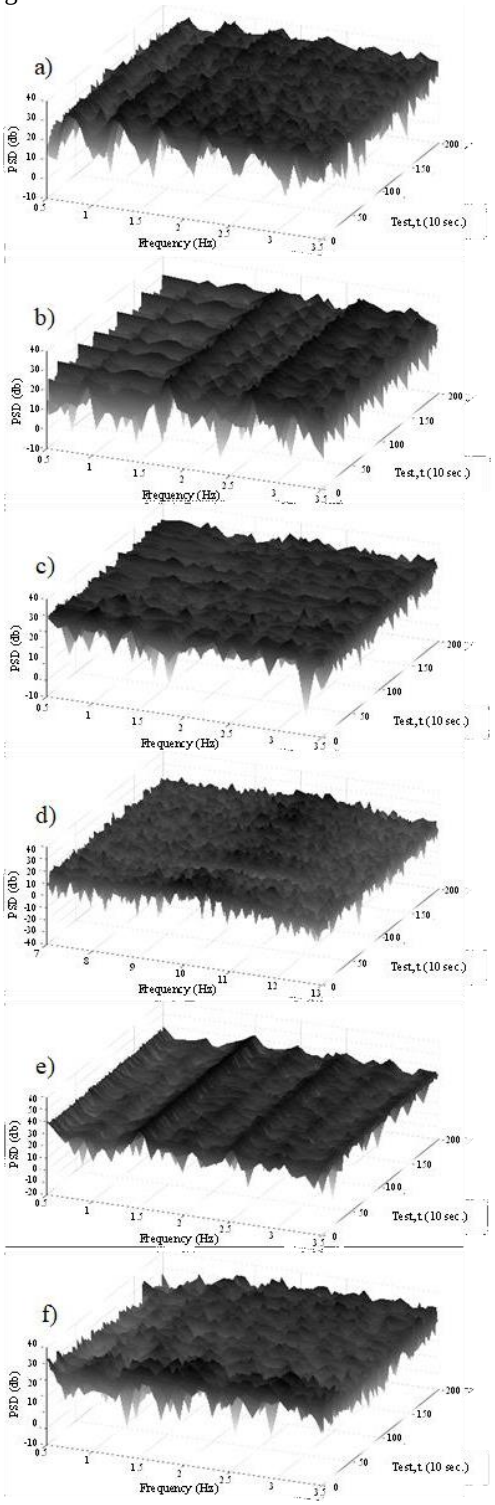

Figure 4: Pseudo-tridimensional graphic of evolution in frequency – Barlett´s Periodogram:a) Opening/Close-Eye, b)Opening/Close-Boca, c) Concentration, d) Meditation, e) Up/Down-Eye y f) Left/Right-Eye

The magnitude in $S_{xx}(F)$ has similar characteristics in $E[P^{B}{}_{xx}(f)]$, the signal with a rectangular window in $E[P^{W}{}_{xx}(f)]$ attenuates the frequency response from $w(n) = 8$ and the 32 windows deforms the frequency response due to the overlapping and averaging of the signals generating a difference between the window result, keeping in mind that the harmonics do not present an ideal model, there is an error of variance in each signal (not studied in this paper) leading to an attenuation of the dominant peaks linearizing the frequency response. Figure 6 (b) represents the same test performing the processing with the WelchPeriodogram with a Hanning window, where signals with higher smoothing are obtained obtaining a lower spectral density in the harmonics. Comparing the results in both windows, a better spectral estimation is obtained by selecting the rectangular window with$w(n) = 4$, the Hanning window making use of 4 windows of the vector
$x(n)$ softens the weights by losing the harmonics. Performing the spectral analysis by applying a samplingfrequency F_s lower than that described in this paper will not present consistent results.

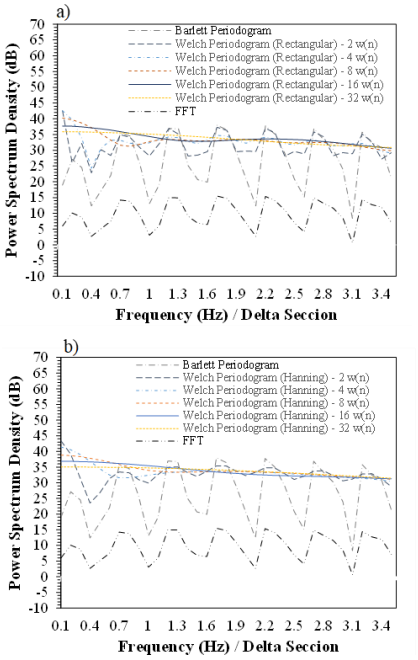

Figure 5: Spectral analysis of subject 1 in movements of Opening/Close – Eye comparing in: (a) FFT, Barlett´s Periodogram, Welch´s Periodogram (Rectangular) with $w(n)$ 2-4-8-16-32 y (b) FFT, Barlett´s Periodogram, Welch´s Periodogram (Hanning) with $w(n)$ 2-4-8-16-32.

3.4. Welch´s Periodogram processing

Developing the modification made by Welch in the Barlett´s Periodogram shown in (23) to (27) where $M = 4$ with a length in the window $L = 1280$, an increase in PSDwas obtained in Figure 7(a) deformation in the frequency response visualizing the 3 harmonics present in Figure 2(a) and Figure 4(a), the range of variation in amplitude decreases compared to the

Industrial Engineering Journal
ISSN: 0970-2555
Volume : 52, No. 2, JULY - DECEMBER 2023

results with Barlett. Figure 7(b) presents weights with wider lobes at frequencies 0.8.1.7 *and* 2.6 *Hz* with noise input at frequencies below0.8 *Hz*. Figure 7(c) presents the immersion of harmonics throughout the course in frequency deforming the resulting average signal. Figure 7 (d) in comparison with Figure 2(d) and Figure 4(d) does not show a significant result, the averaging of the windows allows the slight smoothing of the frequency weighted in the Alpha section, such as the harmonics are within 9 to 12 *Hz*. Figure 7 (e) presents deformations in frequency in the 1.5 and 2.5*Hz* harmonics, the frequencies shown are displayed correctly with smoothed lobes. Figure 7(f) presents harmonic dives at frequencies below 1.1 *Hz* obtaining the result compared with Figure 2(f) and Figure 4(f).Figure 8 presents the results in the pseudo-dimensional graphs applying Welch's Periodogram processing with a rectangular window. The temporal evolution remains constant in the movement tests Opening / Closing - Eye, Opening / Closing - Mouth, Up / Down - Eye and left / Right - Eye comparing the results with Figures. 5 and 3, the modification observed in Figures 8(c) and (f) are shown throughout the temporal evolution at frequencies lower than 2 *Hz* in the concentration decreasing the amplitude with increasing frequency.

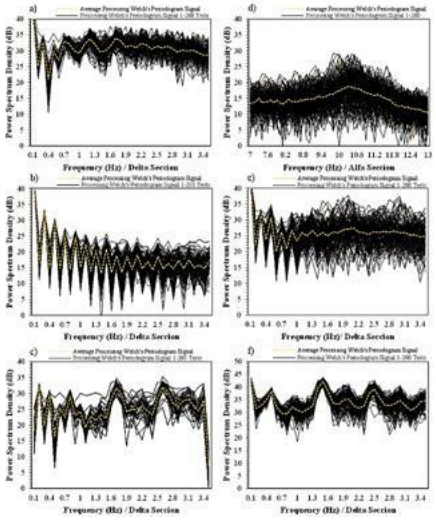

Figure 6: Processing by applying Welch´s Periodogram (Rectangular) $w(n)$ = 2 in 6 movements in 200 tests in 10-second periods (N=5120,0.5≤Δ≤3.5 Hz, 7≤α≤13 Hz-Meditation): a) Opening/Close-Eye, b) Opening/Close-Boca, c) Concentration, d) Meditation, e) Up/Down-Eye y f) Left/Right-Eye

3.5. Comparison of analysis in frequency response

In this subsection, the components of maximum values are shown in each movement applying the 3 techniques shown previously. Figure8 shows the time evolution of the maximum amplitude values in frequency corresponding to 2000 seconds of observation by movement, it is visualized that the algorithm of the FFT and Bartlett's Periodogram maintains in most movements identical frequency amplitudes [21]. Figure 9 (a) specifies the movement of Opening / Closing of Eyes visualizing consecutive patterns in 1.2 *and* 1.7 *Hz* in the methods of the FFT and Barlett's Periodogram while applying the Welch Periodogram technique is obtained in 0.8 and 1.3 *Hz* The Figure9(b) presents a harmonic in 2.7 *Hz* in the FFT and Barlett's Periodogram while the Welch's Periodogram is offset by obtaining it in the 2.3 Hz harmonic. Figure9(c) presents a maximum amplitude scattering in the FFT and Bartlett's Periodogram not presenting a definite time evolution, relating the results with Figures 2(c), 5(c) and 9(c), the Welch Periodogram shows a weighting frequency of 0.1 *Hz*, the result of an averaging of the variant samples, the result is obtained given the smoothing of the spectrum. Figure9(e) shows 1 harmonic defined in 1.5 *Hz* generated by theFFT and Bartlett, applying the spectral estimation technique of the Welch Periodogram visualizes a harmonic environment at 1.1 *Hz*. Figure9(f) presents a recreation not relating a constant pattern around a reference frequency in the FFT and Barlett technique, the Welch technique presents a component in frequency 0.1 *Hz* similar to Figure9(c) agreed with [22] the frequency weights with pseudo-three-dimensional graphics visualize the pattern obtained with Welch's Periodogram. The segment deformed in frequency in the temporal evolution in the Concentration test allows defining in detail a frequency of recognition, considering in the study that the harmonics do not present a notorious definition in a real situation, it is allowed to apply the Welch Periodogram determining if the subject is concentrated.

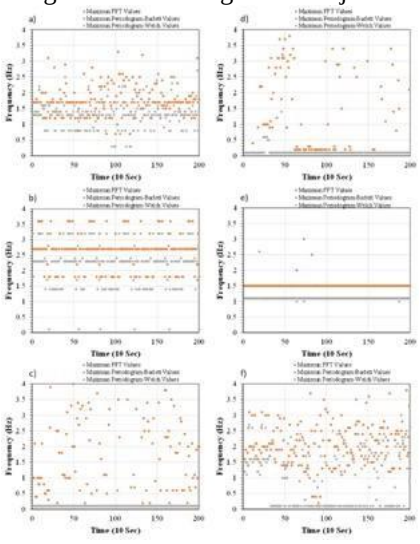

0.2

Figure 8: Two-dimensional diagram representing the evolution of maximum magnitudes in 2000 seconds of test: a) Opening/Close-Eye, b) Opening/Close-Boca, c) Concentration, d) Meditation, e) Up/Down-Eye y f) Left/Right-Eye.

application of non-parametric techniques. The set of tests was carried out applying spectral analysis showing the evolution in frequency, magnitude-frequency relation, and average frequency. The obtained result showed harmonics found in fixed frequencies in the movements of Opening / Closing-Mouth, Opening / Closing-Eye, Eye Movement Up / Down, and Left / Right Eye Movement, applying the FFT processing technique, Bartlett Periodogram with two segments and Welch Periodogram with rectangular window not overlapping. The elimination of the variance within the data set must be stipulated correctly avoiding the elimination of harmonics. The methods showed a good performance referring to the measurement point N_z , it is not intended to obtain a similar resultunder different conditions. Barlett's

4. Conclusion

In this study, the comprehensive analysis of 6 basic actions carried out daily has been proposed, presenting together the

Industrial Engineering Journal
ISSN: 0970-2555
Volume : 52, No. 2, JULY - DECEMBER 2023

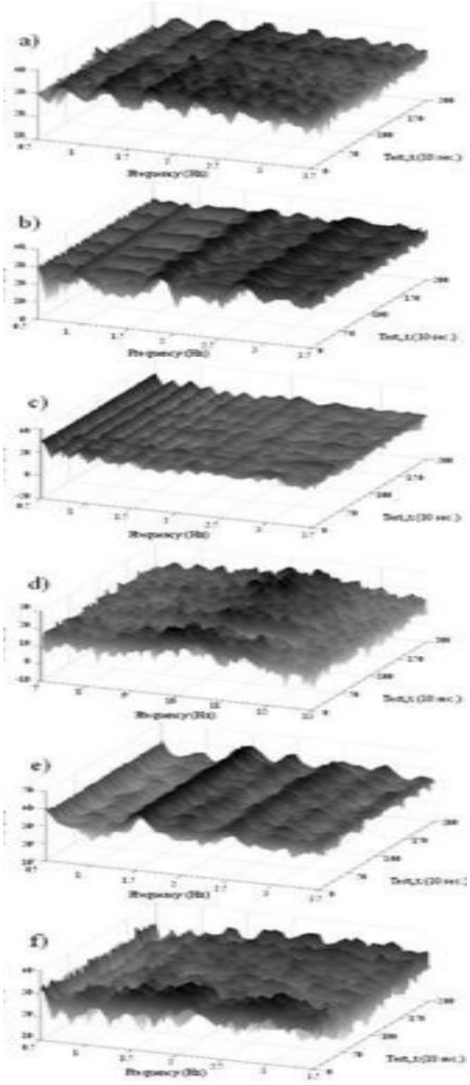

Figure 9: Pseudo-tridimensional graphic of evolution in frequency – Welch´s Periodogram: a) Opening/Close-Eye, b) Opening/Close-Mouth, c) Concentration, d) Meditation, e) Up/Down-Eye y f) Left/Right-Eye.

Periodogram and FFT techniques presented consistent results in the search for patterns located in the Delta biosignal range. The set of two-dimensional magnitude-frequency graphs showed variance in the dispersion of harmonics by test in the Concentration and Meditation, in the latter a constant operating range is visualized, finding the most harmonics with maximum magnitude. The Welch´s Periodogram by applying 4 non-overlapping rectangular windows is not optimal for the tests performed. By contemplating the real frequency response of the concentration, it is possible to apply the third method allowing using a non-real weighted frequency the determination of a concentrated subject.

Acknowledgment
The tests were carried out in the Instituto Tecnológico de Minatitlán using its installations and resources in the Electronics Engineer area.

References

[1] C. Dissanyaka, D. Cvetkovic, B. Ahmed, H. Abdullah y T. Penzel, «Classification of Healthy and Insomnia Subjects Based on Wake-to-Sleep Transition,» IEEE, p. DOI: 11.1109/IECBES.2016.7843497, 06 February 2017.

[2] Y. Li, M.-Y. Lei, Y. Guo, Z. Hu y H.-L. Wei, «Time-Varying Nonlinear Causality Detection Using Regularized Orthogonal Least Squares and Multi-Wavelets With Applications to EEG,» IEEE Access, vol. 6, nº DOI: 10.1109, pp. 17826 - 1840, March26,2018.

[3] S. N. Farihah, K. Y. Lee, W. Mansor, N. B. Mohamad, Z. Mahmoodin y S. A. Saidi, «EEG average FFT index for dyslexic children with writing disorder,» IEEE, vol. DOI: 10.1109/ISSBES.2015.7435880, pp. 118- 121, 21 March 2016.

[4] D. Seth, D. Chakraborty, P. Ghosal y S. K. Sanyal, «Brain Computer Interfacing: A Spectrum Estimation Based Neurophysiological Signal Interpretation,» IEEE, p. DOI: 10.1109/SPIN.2017.8050008, 28 September 2017.

[5] Srinath, R., & Gayathri, R. (2020). Detection and classification of electroencephalogram signals for epilepsy disease using machine learning methods. Int. J. Imaging Syst. Technol., doi: https://doi.org/10.1002/ima.22486.

[6] N. Sulaiman, M. N. Taib, S. Lias y Z. H. Murat, «Development of EEG-Based Stress index,» IEEE, p. DOI: 10.1109/ICoBE.2012.6179059, 05 April 2012.

[7] H. Yoshida, H. Kuramoto, Y. Sunada y S. Kikkawa, «EEG Analysis in Wakefulness Maintenance State against Sleepiness by Instantaneous Equivalent Bandwidths,» IEEE, p. DOI: 10.1109/IEMBS.2007.4352212, 22 October 2007.

[8] R. Velnath, V. Prabhu, y S. Krishnakumar, «Analysis of EEG Signal for the Estimation of Concentration Level of Humans», *IOP Conf. Ser. Mater. Sci. Eng.*,vol. 1084, n.º 1, p. 012003, mar. 2021, DOI: 10.1088/1757-899x/1084/1/012003.

[9] M. M. Hasan, M. H. Sohag y M. Ahmad, «EEG Biometrics Based on Small Intra-individual and large Inter-individual Difference of Extracted Features,» IEEE, p. DOI: 10.1109/ICECTE.2016.7879629, 16 March 2017.

[10] C. Ming, G. Xiaorong, G. Shangkai y W. Boliang, «Stimulation Frequency Extraction in SSVEP-Based Brain-Computer Interface,» IEEE, p. DOI: 10.1109/ICNIC.2005.1499843, 29 August 2005.

[11] A. Isaksson, A. Wennberg y L. Zetterberg, «Computer Analysis of EEF Signals with Parametric Models,» Proceedings of the IEEE, vol. 69, nº 4, pp. 451-461, April 1981.

[12] M. P. Tarvainen, J. K. Hiltunen, P. O. Ranta-aho y P. A. Karjalainen, «Estimation of Nonstationary EEG With Kalman Smoother Approach: An Application to Event-Related Synchronization(ERS),» IEEE Transactions on Biomedical Engineering, vol. 51, nº 3, pp. 516 - 524, March 2004.

[13] Moreno Escobar, J. J., Morales Matamoros, O., Aguilar del Villar, E. Y., Tejeida Padilla, R., Lina Reyes, I., Espinoza Zambrano, B., Luna Gómez, B. D., & Calderón Morfín, V. H. (2021). Non-Parametric Evaluation Methods of the Brain Activity of a Bottlenose Dolphin during an Assisted Therapy. Animals, vol. 11, n.o 2, doi: 10.3390/ani11020417.

[14] D.K.Reddy, A.Manglick, R.Upadhyay y P. Padhy, «Feature Extraction and Classification of Electroencephalogram Signals for Vigilance Level Detection,» IEEE, p. DOI: 10.1109/CARE.2013.6733720, 10 February 2014.

[15] M. Murugappan y S. Murugappan, «Human Emotion Recognition Through Short Time Electroencephalogram (EEG) Signals Using Fast Fourier Transform (FFT),» IEEE, p. DOI: 10.1109/CSPA.2013.6530058, 13 June 2013.

[16] Z. Feng y Z. Xu, «Analysis of Rat Electroencephalogram under Slow Wave Sleep Using Wavelet Transform,» IEEE, p. DOI: 10.1109/IEMBS.2002.1134404, 06 January 2003.

[17] J. G. Sled, A. P. Zijdenbos y A. C. Evans, «A Nonparametric Method for Automatic Correction of Intensity Nonuniformity in MRI Data,» IEEE Transactions on Medical Imaging, vol. 17, nº 1, pp. 87-97, February 1998.

[18] S. Lisha y S. Minfen, «Analysis of non-stationary electroencephalogram using the wavelet transformation,» IEEE, vol. DOI: 10.1109/ICOSP.2002.1180084, pp. 26-30, 28 February2003.

[19] A. Liavas, G. Moustakides, G. Henning, E. Psarakis y P. Husar, «A Periodogram-Based Method for the Detection of Steady-State Visually Evoked potentials,» IEEE Transactions, vol. 45, nº 2, pp. 242-248,February 1998.

[20] R. Upadhyay, P. K. Kankar, P. K. Padhy y V. K. Gupta, «Extraction and Classification of Electroencephalogram signals,» IEEE, p. DOI: 10.1109/ICCIC.2012.6510216, 02 May 2013.

[21] A. Vyas y G. Mishra, «Classification of Two Mental States Using,» IEEE, p. DOI: 10.1109/CARE.2013.6733769, 10 February 2014.

[22] F. He, S. A. Billings, H.-L. Wei, P. G. Sarrigiannis y

[23] Y. Zhao, «Spectral Analysis for Nonstationary and Nonlinear Systems:

[24] A Discrete-Time-model-based Approach,» IEEE Transactions, vol. 6, nº 8, pp. 2233- 2241, August 2013.

[25] Y. Takizawa, S. U. Makio Ishiguro y A. Fukasawa, «Analysis of Brain Electroencephalograms With The Instantaneous Maximun Entropy Method,» IEEE, 23 April 2015.

[26] S. M. S. A. Unde, M. Revati, «Coherence Analysis Of EEG Signal Using Power Spectral Density,» IEEE, p. DOI: 10.1109/CSNT.2014.181, 29 May 2014

Author Profile

José de Jesús Moreno Vázquez, he obtained a B. S degree in Electronic Engineering from the Instituto Tecnológico de Minatitlán, Veracruz, Mexico, in 1995. He received the MSc degree from the Centro Nacional de Investigación y Desarrollo Tecnológico National (CENIDET) in 1996 and the Ph. D. degree in Bioengineering from the Universidad Politécnica de Valencia in 2011. He is currently head of research projects in the Department of Electronic Engineering and professor of the Master's degree in Electronic Engineering. His current interests are digital systems, digital signal processing, bioelectronics, and instrumentation.

Aldo Rafael Sartorius Castellanos, he received the B. S degree in Electromechanical Engineering from the Universidad Veracruzana (UV) in 2000. He received the MSc and Ph. D. degrees in Automatics from the Universidad Central de las Villas (UCLV) in 2002 and 2005, respectively. He currently works as a full-time Professor at the Tecnológico Nacional de México campus, Instituto Tecnológico de Minatitlán (TecNM / ITM) and collaborates as a visiting professor at the Centro de Tecnología Avanzada (CIATEQ). His research lines are focused on the automation and control of electromechanical systems using embedded systems.

Marcia Lorena Hernández Nieto, she obtained a B. S degree in Electronic Engineering from the Instituto Tecnológico de Minatitlan, Veracruz, Mexico, in 1994. She received the MSc degree from the Centro Nacional de Investigación y Desarrollo Tecnológico National (CENIDET). She is currently a professor in the department of electronic engineering and the Master's degree in electronic engineering. Her areas of interest are in power electronics.

Antonia Zamudio Radilla, obtained her Electronic Engineer title from the Instituto Tecnológico de Minatitlan, Veracruz Mexico in 1996. Master in University Teaching from the Universidad Iberoamericana Golfo Centro, Puebla, Mexico, in 2012. She is currently assigned to the Department of electronic engineering. She is a professor of the Master's Degree in Electronic Engineering and the Bachelor's Degree in Electronic Engineering at I.T. from Minatitlan.

Bryan QuinoOrtíz, He is a student of electronic engineering at the Instituto Tecnológico de Minatitlan, Veracruz, Mexico. His current interests are digital systems, digital signal processing, bioelectronics.